FULLY RENEWABLE THERMOSETS BASED ON BIS-EUGENOL PREPARED BY THIOL-CLICK CHEMISTRY

Dailyn Guzmán,[1] Angels Serra,[1,2]* Xavier Ramis,[3] Xavier Fernández-Francos,[3] Silvia De la Flor[4]

[1] Centre Tecnològic de la Química de Catalunya, CTQC, C/Marcel·lí Domingo s/n Edifici N5, 43007, Tarragona, Spain.

[2] Department of Analytical and Organic Chemistry, Universitat Rovira i Virgili, C/ Marcel·lí Domingo s/n, Edifici N4, 43007, Tarragona, Spain.

[3] Thermodynamics Laboratory, ETSEIB Universitat Politècnica de Catalunya, Av. Diagonal 647, 08028, Barcelona, Spain.

[4] Department of Mechanical Engineering, Universitat Rovira i Virgili, C/ Països Catalans 26 43007, Tarragona, Spain.

* Corresponding author: E-mail: angels.serra@urv.cat Telf: 0034-977559558

Abstract

Thiol-ene photocuring and thiol-epoxy thermal curing have been applied to prepare new thermosets from renewable substrates. As monomers, a tetrallyl and a tetraepoxy derivative of bis-eugenol were prepared by dimerization of eugenol, allylation and further epoxidation. These compounds were reacted with a commercially available tetrathiol, PETMP, and thiols synthesized from two natural resources as squalene (6SH-SQ) and eugenol (3SH-EU) in photoinitiated and thermal conditions. The reaction process was studied by calorimetry, and the materials obtained were characterized by thermogravimetry, thermomechanical studies and mechanical testing. Thiol-epoxy materials showed a better mechanical performance than thiol-ene

photocured thermosets. This new epoxy monomer of renewable origin allowed to prepare materials with final properties better than those obtained from the diglycidylether of bisphenol A, owing to the high functionality of bis-eugenol and its rigid and compact structure.

Keywords: Green chemistry, bis-eugenol, click reaction, thiol-epoxy, thiol-ene.

1. Introduction

The declining oil reserves, global warming, and littering problems threaten the future of polymeric materials. For these reasons, we need to transform the petrochemical era into a new green with new polymeric materials derived from renewable resources that match the performance of their petrochemical counterparts.[1]

Amongst renewable starting materials, vegetable natural oils have been widely used to prepare thermosetting materials. However, their flexible aliphatic structure limits their range of application since the materials obtained usually present too low T_gs.[2,3,4] Some authors reported on the use of renewable alternatives to plant oils for obtaining thermosets.[5] This is the case of vanillin,[6,7] itaconic acid,[8] cardanol,[9] furan derivatives[10] or sugars,[11] among natural starting substances. From them, different materials with good mechanical performances were obtained because of the more rigid structure of the network formed. Therefore, the proper selection of the monomer structure is of special interest to reach the desired characteristics.

Eugenol (EU, 4-allyl-2-methoxyphenol) is the main component (80-90%) of clove oil.[12] This compound has pharmaceutical applications, since it can act as antimicrobial, analgesic, antioxidant, anti-inflammatory, antispasmodic, antigenotoxic, anticarcinogenic and antidepressant.[13,14,15] It is also used as flavour and fragance in

cosmetics and food industry.[16] Eugenol was classified as “generally recognized as safe (GRAS)” by the US Food and Drug Administration.[17]

Structurally, eugenol is an aromatic compound with two functional groups, phenol and allyl that can be further modified to prepare a great variety of derivatives.[18,19] Some researchers have selected several eugenol-based compounds for preparing thermosets. An epoxy derivative of eugenol was crosslinked by an anhydride derived from rosin and the thermosets prepared have similar reactivity, dynamic mechanical properties and thermal stability as commercial materials.[20] Wan et al.[21] prepared a new epoxy material with a bio-based content of 70.2% wt. from a eugenol derivative cured by 4,4’-diamino diphenyl methane. The new material had a T_g of 114 °C, 40 °C lower than the diglycidylether of bisphenol A (DGEBA) based material. Nevertheless, the new epoxy-eugenol thermoset had higher Young’s modulus and hardness than the petrochemical analogue. In another study, highly stiff epoxy thermosets derived from eugenol with a triazine core structure and three epoxy groups per molecule was prepared and then cured by using 3,3’-diamino diphenylsulfone.[22] In comparison with DGEBA thermosets cured under the same conditions, the new eugenol-based material led to improved thermomechanical properties (33 °C in T_g, 39% in Young’s modulus and 55% enhancement in hardness). Recently, an epoxy derivative of eugenol has been used for the preparation of vitrimeric materials. The epoxy eugenol was reacted with succinic anhydride in different proportions and the materials obtained showed excellent properties of shape memory and crack healing.[23]

In addition to the transformation of eugenol to epoxy monomers, the presence of allyl groups and phenol opens the possibility of using eugenol derivatives as monomers in the preparation of three-dimensional structures by thiol-ene processes. Yoshimura

et al.[24] prepared triallyl eugenol, which was crosslinked through a photochemical thiol-ene process leading to adhesives with a low T_g of 9.1 °C. The unexpected low T_g was explained by the occurrence of side-reactions during the thiol-ene process, such as thiol-thiol coupling that hinders the complete reaction to occur. In a previous work of our group, we could prove that the substitution of an allyl group of triallyl eugenol by a glycidyl group allowed to increase the T_g value and enhance the mechanical performance in reference to the thiol-ene material.[25] Thus, thiol-ene and thiol-epoxy click reactions can lead to very different materials even when the structure of the starting monomers is similar.

The possibility of dimerization of eugenol[26] opens the possibility to prepare phenols that approach the structure of the bisphenol A molecule.[27] From bis-eugenol derivatives, thermosets with higher thermomechanical performance could be prepared as green alternatives to petrochemical materials, following two different methodologies: a) photoinitiated thiol-ene and b) thermal thiol-epoxy curing processes. This is because of bis-eugenol can be allylated to get tetra allyl bis-eugenol (4A-BEU)[28] and subsequently allyl groups can be transformed into glycidylic groups by epoxidation to obtain a tetraglycidyl bis-eugenol (4EPO-BEU). In the present work, both tetrafunctional compounds have been prepared and then crosslinked with various thiol compounds to obtain materials with different three-dimensional network structures. As thiol crosslinkers we selected pentaerythritol tetrakis (3-mercaptopropionate) (PETMP), the trithiol synthetized from eugenol (3SH-EU) and the hexathiol derived from squalene (6SH-SQ), all compounds with the possibility to be obtained from renewable resources. All the starting materials are represented in Scheme 1.

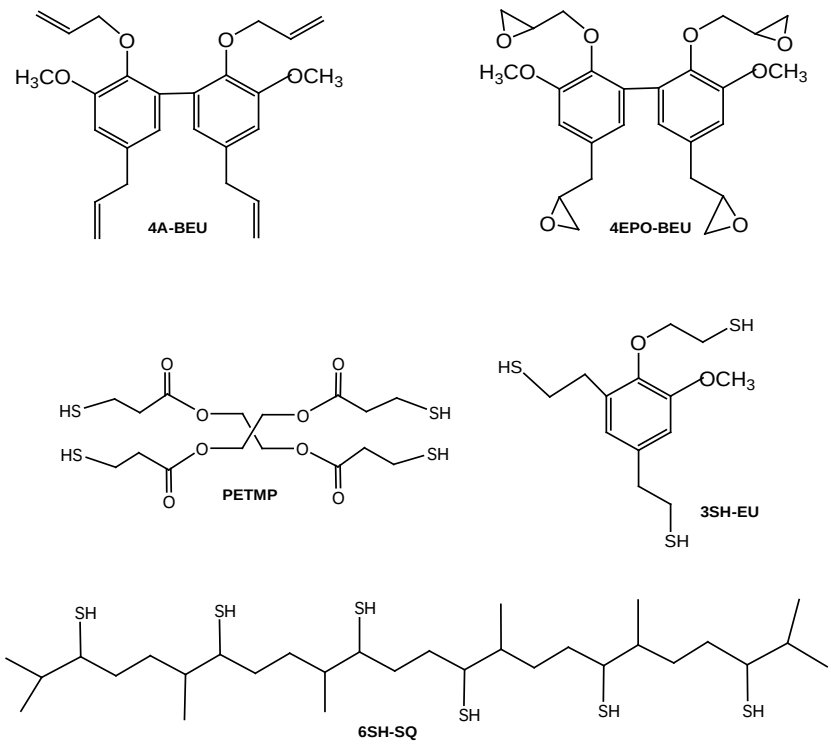

Scheme 1. Chemical structures of the starting compounds

The curing procedure has been monitored by calorimetry (DSC) and infrared spectroscopy (FTIR) to find out the best reaction conditions. The fully bio-based thermosets obtained have been characterized by thermogravimetry, thermomechanical analysis and mechanical tests.

2. Experimental part

2.1. Materials

Eugenol (EU), allyl bromide, thioacetic acid (TAA), 2,2-dimethoxy-2-phenylacetophenone (DMPA), 4-(N,N-dimethylamino)pyridine (DMAP), 1-methylimidazole (1-MI), pentaerythritol tetrakis (3-mercaptopropionate) (PETMP), squalene (SQ) and oxone (potassium peroxo monosulphate) were purchased from Sigma-Aldrich and were used without further purification. Potassium hexaferricyanide,

ammonium hydroxide and inorganic salts from Scharlab were used as received. Benzyl triethyl ammonium chloride (TEBAC) was purchased from Alfa Aesar. Methanol, acetone, ethyl acetate and N,N-dimethylformamide (DMF) from VWR were purified by standard procedures.

2.2. Preparation of starting products

2.2.1. Synthesis of bis-eugenol (BEU)

The synthesis of bis-eugenol was based on a previous reported procedure. In a 500 mL flask, 10.5 g (64.0 mmol) of eugenol were dissolved in a mixture of 100 mL of acetone and 50 mL of water and then 70 mL of NH_4OH at 25 wt. % were added under magnetic stirring. The mixture was maintained for 10 min while a green-yellow colour appeared. To this mixture a saturated aqueous solution of $K_3[Fe(CN)_6]$ (21.1 g, 64.0 mmol) was added dropwise during 5 h. When finished, 70 mL of NH_4OH at wt. 25% were added to keep the alkalinity of the reaction medium and the mixture was kept on stirring overnight. The solution was lead to pH 7 by adding a 1M solution of HCl at room temperature. The solid product that appeared was filtered, washed three times with distilled water and then dried in the vacuum oven at 60 °C. The product was purified by column chromatography using a mixture of ethyl acetate/hexane (40/60) as eluent. Yield: 10.3 g (98%) (m.p. 104 °C by DSC). ^{1}H NMR ($CDCl_3$, δ in ppm): 3.33 (d, 4H, J=6.5 Hz, -CH_2-), 3.79 (s, 6H, -OCH_3), 4.96-5.18 (m, 4H, =CH_2), 6.14 (m, 2H, =CH-) and 6.69-6.75 (m, 4H, aromatic). ^{13}C NMR ($CDCl_3$, δ in ppm): 40.0 (-CH_2-), 56.0 (-OCH_3), 110.8 (ar, C-6), 115.6 (=CH_2), 123.3 (ar, C-2), 124.7 (ar, C-3), 131.8 (ar, C-1), 137.8 (=CH-), 141.2 (ar, C-4) and 147.4 (ar, C-5).

2.2.2. Synthesis of tetra allyl derivative of bis-eugenol (4A-BEU)

The synthesis of tetra allyl biseugenol was based on a previous reported procedure.[28] In a 100 mL three-necked flask equipped with magnetic stirrer, thermometer and addition funnel, 5.71 g (17.5 mmol) of BEU and 1.54 g (38.5 mmol) of NaOH were dissolved into 50 mL of DMF. The solution was stirred for 10 min and 4.67 g (38.5 mmol) of allyl bromide was added dropwise during 1 h at 40 °C. The mixture was maintained at 40 °C for 3 h and at 70 °C for 30 min. Distilled water was added to dissolve the NaBr formed and the organic product was extracted with chloroform. The organic layer was washed twice with water and dried over $MgSO_4$. The solution was concentrated in the rotavap, dried at high vacuum and then purified by column chromatography using ethyl acetate/hexane (30/70) as eluent. The product obtained was a yellow oil 6.7 g (94% of yield). ^{1}H NMR ($CDCl_3$, δ in ppm): 3.3 (d, 4H, J=6.5 Hz, -CH_2-), 3.87 (s, 6H, -OCH_3), 4.29 (d, 4H, J=6.3 Hz, -CH_2-O-), 4.99-5.12 (m, 8H, =CH_2), 5.75-5.85 (m, 2H, =CH-), 5.92-6.02 (m, 2H, =CH-), 6.71 (d, 2H, J=2 Hz, aromatic) and 6.75 (d, 2H, J=2 Hz, aromatic). ^{13}C NMR ($CDCl_3$, δ in ppm): 39.8 (-CH_2-), 55.6 (-OCH_3), 73.7 (-CH_2-O-), 111.5 (ar, C-3), 115.6 (=CH_2), 116.4 (=CH_2), 123.2 (ar, C-5), 132.5 (ar, C-4), 134.4 (=CH-), 134.7 (=CH-), 137.2 (ar, C-6), 143.8 (ar, C-1) and 152.4 (ar, C-2). FTIR-ATR: 3076, 3000, 2976, 2837, 1680, 1638, 1580, 1484, 1460, 1417, 1355, 1267, 1218, 1142, 1100, 1047, 988, 912, 844, 814, 748 and 722 cm^{-1}.

2.2.3. Synthesis of tetraglycidyl derivative of bis-eugenol (4EPO-BEU)

In a three-necked 1000 mL flask equipped with magnetic stirrer and addition funnel, 1 g of 4A-BEU (2.5 mmol) was dissolved in 100 mL of ethyl acetate and 100 mL of acetone. Then, a solution of 34.14 g of $NaHCO_3$ (0.41 mol) and 0.12 g (0.53

mmol) of benzyl triethyl ammonium chloride in 70 mL of water was added. The mixture was cooled down at 5-8 °C under vigorous stirring and a solution of oxone (45 g, 73.8 mmol) in 150 mL of water was added dropwise for 2 h, approximately. The mixture was kept at room temperature under stirring for 3 days. Once finished, the phases were separated, and the organic layer washed twice with water. After drying over $MgSO_4$, the solvent was evaporated in the rotavap. The product was purified by column chromatography using ethyl acetate/hexane mixture (60/40) as eluent. 1 g of a viscous yellow liquid was obtained (86 % yield). ^{1}H NMR ($CDCl_3$, δ in ppm) (see Figures 1 and 2): 6.81-6.77 m (ar, 4H), 3.95 and 3.92 m (-CH_2-O-, 4H), 3.89 s (CH_3-O-, 6H), 3.16 m (CH of glycidyl groups attached to Ph, 2H), 3.04 m (CH of glycidyl ether, 2H), 2.79 pm (CH_2 of glycidyl groups attached to Ph), 2.75-2.51 m (-CH_2- of oxirane rings, 8H) and 2.59-2.34 m (-CH_2- of glycidyl groups directly attached to Ph, 4H).^{13}C NMR ($CDCl_3$, δ in ppm) (see Figure 3 and 4): 38.1 (-CH_2-), 44.0 (-CH_2- oxirane), 46.4 (-CH_2- oxirane), 50.1 (CH- oxirane), 52.0 (CH- oxirane), 55.5 (-OCH_3), 73.5 (-CH_2-O-), 112.2 (ar, C-3), 123.1 (ar, C-5), 132.0 (ar, C-4), 132.4 (ar, C-6), 143.9 (ar, C-1) and 152.0 (ar, C-2). FTIR-ATR: 3052, 2996, 2935, 2841, 1719, 1581, 1484, 1460, 1417, 1359, 1255, 1220, 1146, 1096, 1046, 1011, 965, 909, 833 and 732 cm^{-1}.

2.2.4. Synthesis of hexathiol from squalene (6SH-SQ)

The product was obtained following a two-step procedure previously reported for Acosta et al.[29] which includes a thiol-ene photochemical reaction of squalene with thioacetic acid in presence of DMPA, followed by a saponification of the thioester groups formed with methanolic NaOH.

2.2.5. Synthesis of trithiol from eugenol (3SH-EU)

The trithiol from eugenol was synthetized following a similar procedure of the hexathiol. The synthesis and characterization of 3SH-EU was described by us in previous work.[30]

2.3. Preparation of the curing mixtures

Two different types of formulations were prepared with the composition detailed in table 1. Thiol-ene formulations named as 4A-BEU/thiol and thiol-epoxy formulations named as 4EPO-BEU/thiol. The mixtures were prepared by mixing the compounds in stoichiometric ratios of allyl/SH and epoxy/SH groups, and were homogenized by hand stirring using a spatula.

Three different thiol-ene formulations were prepared from 4A-BEU as allyl monomer and three different thiols: PETMP, 3SH-EU and 6SH-SQ. The photochemical reaction was catalyzed by adding 4 phr (parts per hundred of mixture) of a mixture of Irgacure 184 and Irgacure 819 in weight ratio 3:1 in some drops of acetone to obtain a homogeneous mixture. Then, acetone was eliminated at vacuum for 30 minutes at room temperature. These formulations were named as 4A-BEU/PETMP; 4A-BEU/3SH-EU and 4A-BEU/6SH-SQ.

Table 1. Percentages in weight of monomers and thiols used in the preparation of the different thiol-ene and thiol-epoxy formulations**.**

Formulation	**thiol** (%)	**allyl** (%)	**epoxy** (%)	**photoinitiator** (%)	**catalyst** (%)
4A-BEU/PETMP	52	44	---	4	---
4A-BEU/3SH-EU	51	45	---	4	---
4A-BEU/6SH-SQ	50	46	---	4	---
4EPO-BEU/PETMP	50	---	49	---	1
4EPO-BEU/3SH-EU	49	---	50	---	1
4EPO-BEU/6SH-SQ	48	---	51	---	1

Three different thiol-epoxy formulations were prepared from tetraepoxy (4EPO-BEU) with the same thiols, PETMP, 3SH-EU and 6SH-SQ. 2 or 8 phr (parts per hundred of epoxy) of 1-MI as catalyst. These formulations were named as 4EPO-BEU/PETMP; 4EPO-BEU/3SH-EU and 4EPO-BEU/6SH-SQ.

2.4. Characterization techniques

^{1}H NMR and ^{13}C NMR spectra were registered at room temperature in a Varian Gemini 400 spectrometer. $CDCl_3$ was used as the solvent. For internal calibration the solvent signal corresponding to $CDCl_3$ was used: δ (^{1}H) = 7.26 ppm, δ (^{13}C) = 77.16 ppm.

The samples of thiol-ene compositions were photocured at 30 °C in a Mettler DSC-821e calorimeter appropriately modified with a Hamamatsu Lightning cure LC5 (Hg–Xe lamp) with two beams, one for the sample side and the other for the reference side. 5 mg samples were cured in open aluminium pans in nitrogen atmosphere. Two scans were performed on each sample to subtract the thermal effect of the radiation. The method used was 2 min to stabilize the temperature, 10 min irradiation and 2 min at rest. The intensity of the light used was 15 mW/cm^2.

The study of the epoxy-thiol thermal curing was performed by differential scanning calorimetry (DSC) in a Mettler DSC-821e apparatus. For dynamic studies, a flow of N_2 at 100 mL/min was used and the weight of the samples for the analysis was 10 mg. The calorimeter was calibrated using an indium standard (heat flow calibration) and an indium-lead-zinc standard (temperature calibration). The studies were performed in the temperature range of 30-250 °C, with a heating rate of 10 K/min.

The glass transition temperatures (T_gs) of the samples after irradiation were determined in dynamic scans at 20 °C/min from -20 °C to 150 °C. The T_gs of the final thermosets were determined after two consecutive heating dynamic scans at 20 °C/min starting at -20 °C in a Mettler DSC-822e device to delete the thermal history. The T_g value was taken as the middle point in the heat capacity step of the glass transition.

A Bruker Vertex 70 FTIR spectrometer equipped with an attenuated total reflection accessory (ATR) (Golden Gate, Specac Ltd. Teknokroma) which is temperature controlled (heated single-reflection diamond ATR crystal) equipped with a liquid nitrogen-cooled mercury-cadmium-telluride (MCT) detector was used to register the FTIR spectra of the mixtures during UV irradiation and fully cured samples. The spectra were registered in the wave number range between 4000 and 600 cm^{-1} with a resolution of 4 cm^{-1} and averaged over 20 scans. UV-curing was performed using a Hamamatsu Lightning cure LC5 (Hg-Xe lamp) with one beam conveniently adapted to the ATR accessory. A wire-wound rod was used to set a sample thickness of 50 μm. OPUS software was used for the analysis of the spectra. The spectra were corrected for the dependence of the penetration depth on the wavelength and normalized with respect to the absorbance of C=C aromatic peaks at 1587 cm^{-1} (neglecting the contribution of the overlapping tiny signal associated with the allyl group). The normalized S-H st. band at 2576 cm^{-1} and the allyl band at 1639 cm^{-1} were integrated and the thiol and allyl conversions after the photocuring (X_{uv}) and after thermal curing (X_{final}) were determined as:

$$X_{UV} = 1 - \frac{A'_{UV}}{A'_0} \qquad (1)$$

$$X_{final} = 1 - \frac{A'_{final}}{A'_0} \qquad (2)$$

Where A'_{UV}, A'_{final} and A'_0 are the normalized area of thiol or allyl bands after photocuring and thermal curing and at the beginning of the curing, respectively.

The thermal stability of cured samples was studied by thermogravimetric analysis (TGA), using a Mettler TGA/SDTA 851e thermobalance. All experiments were conducted under inert atmosphere (N_2 at 100 mL/min). Pieces of the cured samples with an approximate mass of 8 mg were degraded between 30 and 600 °C at a heating rate of 10 K/min.

Dynamic mechanical thermal analyses (DMTA) were carried out with a TA Instruments DMA Q800 analyzer. Prismatic rectangular samples (40 mm x 6.7 mm x 1.6 mm) of the thiol-ene formulations were prepared by pouring the mixtures in silicone moulds covered with glass slides, which were photoirradiated in an ultraviolet camera (320-390 nm), DymaxECE 2000 UV model systems. The samples were irradiated with an intensity of 105 mW/cm^2 for a period of 60 seconds each face 14 times, waiting for 60 seconds between irradiations to control the temperature of the sample. The thiol-epoxy mixtures from the selected formulations were isothermally cured in a prismatic mould as follows: a) 90 °C for 1 h, with a post curing at 130 °C for 30 min in case of 4EPO-BEU/PETMP and b) 110 °C for 1 h with a post curing at 160 °C for 30 min for 4EPO-BEU/3SH-EU and 4EPO-BEU/6SH-SQ. Three-point bending clamp was used on the prismatic rectangular samples. The samples were first heated at 5 K/min from 30 to 190 °C to erase the thermal history and subsequently analyzed at 3 K/min from 30 to 190 °C at a frequency of 1 Hz with and oscillation amplitude of

10 µm for materials derivative from 4EPO-BEU and at 3 K/min from -20 to 120°C for materials from 4A-EU.

Young's modulus was determined under flexural conditions at 30 °C, with the same clamp and geometry samples, applying a force ramp at constant load rate of 3 N/min, from 0.001 N to 18 N. Three samples of each material were analyzed and the results were averaged. Stress strain at break tests were performed with the film-tension clamp in force-controlled mode. Dog-bone samples were used at a force rate of 1 N/min and the mean value of at least three different samples were reported.

For 4EPO-BEU samples, microindentation hardness was measured with a Wilson Wolpert 401 MAV device following the ASTM E384-16 standard procedure. For each material 10 determinations were made with a confidence level of 95%. The Vickers microindentation hardness number (*HV*) was calculated by the following equation:

$$HV = \frac{1.8544 \, . F}{d^2} \qquad (3)$$

where, *F* is the load applied to the indenter in kgf and *d* is the arithmetic mean of the length of the two diagonals of the surface area of the indentation measured after load removal in mm.

For 4A-BEU samples, due to their elastomeric behaviour, Shore hardness was used for determining their hardness properties. Shore Hardness measures the resistance of the materials to penetration of a spring-loaded needle-like indenter and provides an empirical value that can be used only for comparative purposes. Two scales were used: Shore A, for softer materials and Shore D, for harder ones. According to ASTM D2240-15e1, the test procedure is as follows: the specimen is placed on a hard flat surface

and the indenter is then pressed into the specimen making sure that it is parallel to the surface. The durometer measures the penetration of the indenter (with and end shape of frustum cone in Shore A and needle pin in Shore D) into the material under specified conditions of force (mass of 1 kg in Shore A and 5 kg in Shore D) and time (1 second in present experiments) at room temperature. The depth of penetration is measured on a scale of 0 (zero penetrations) to 100 (maximum hardness value). Samples of, at least, 6 mm in thickness and 25 mm in width/length, with flat and parallel surfaces were used. Ten measurements were done in each specimen and the average result is presented.

3. Results and Discussion

3.1. Synthesis and characterization of starting monomers

In the present study, we firstly prepared bis-eugenol (BEU) by a previously published procedure,[26] which is based on the oxidative coupling of eugenol produced by the redox ferricyanide-ferrocyanide system. It should be commented that apart from the chemical synthesis, a biological synthesis for BEU using Kalopanax Pictus Callus culture has been published, which leads to a pure product without any side-reaction.[31] Although advantageous, the biological synthesis falls out of our field of expertise and consequently the classical oxidative coupling of EU has been selected to prepare BEU.

The synthesis of the tetra allyl derivative of bis-eugenol (4A-BEU) was addressed by the procedure depicted in Scheme 2 that consists in the reaction of BEU with allyl bromide. The same compound was obtained by Neda et al.[28] in DMSO solution, but in our case DMF was selected as the reaction solvent and a better yield was obtained.

The structure and purity of the products were determined by NMR spectroscopy. The ^{1}H NMR spectrum is similar to the one reported in the Neda's publication. The ^{1}H and ^{13}C NMR spectra of 4A-BEU are collected in the supporting information.

From the tetra allyl derivative, the corresponding tetra epoxy compound (4EPO-BEU) was easily prepared. The methodology for the epoxidation of the allyl derived from the bis-eugenol, was based on the use of oxone in a biphasic system constituted by a mixture acetyl acetate/water.[32] The oxone method was chosen instead of epoxidation with m-chloroperbenzoic acid, because of its environmental-friendly character.[33]

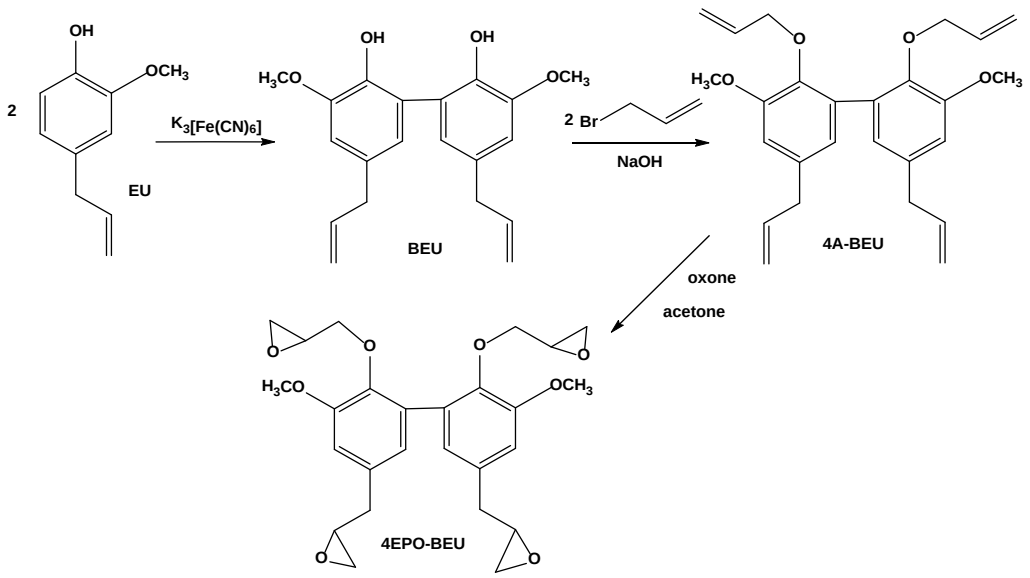

Scheme 2. Synthetic procedure to access the starting monomers.

The epoxidation with oxone requires the use of acetone, since it allows the formation of dioxirane, which is the true epoxidation agent. Applying this method, we obtained the pure tetra epoxy derivative of eugenol (4EPO-BEU) in 86% of yield after purification by column chromatography.

The epoxidated bis-eugenol derivative prepared was characterized by NMR spectroscopy. The following figures correspond to its ^{1}H NMR spectra with the corresponding assignments. Figure 1 present the monodimensional ^{1}H NMR spectrum and figure 2 the ^{1}H-^{1}H COSY correlation spectrum.

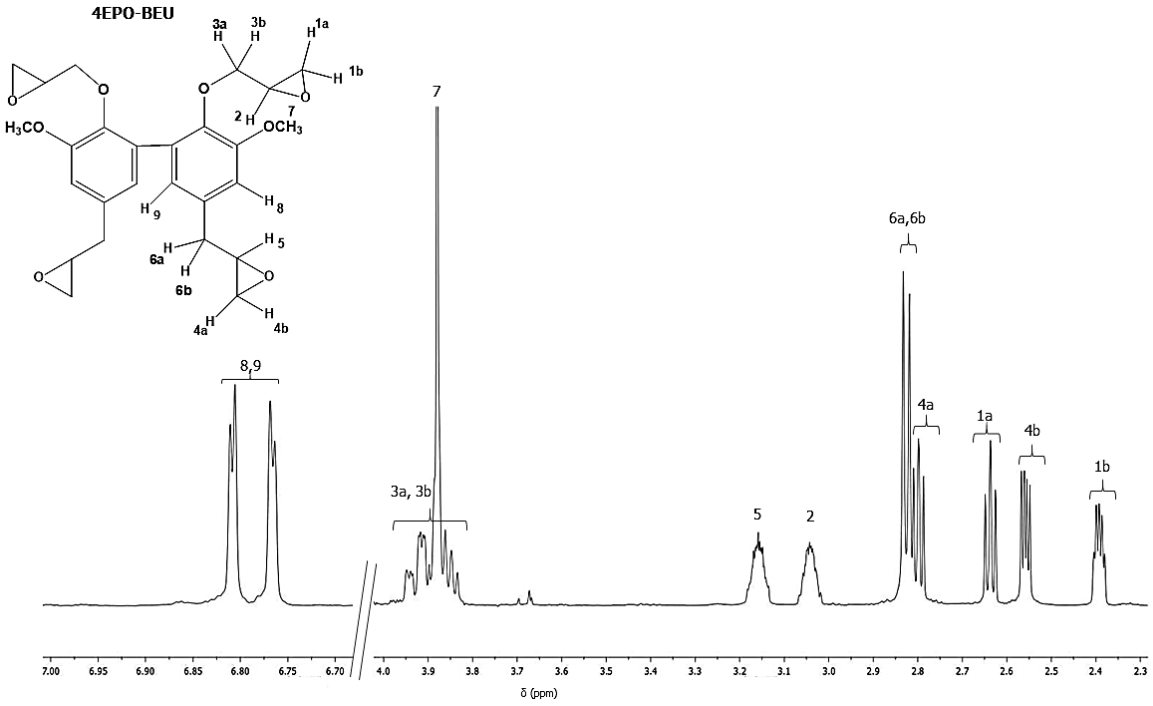

Figure 1. ^{1}H NMR spectrum of 4EPO-BEU in $CDCl_3$.

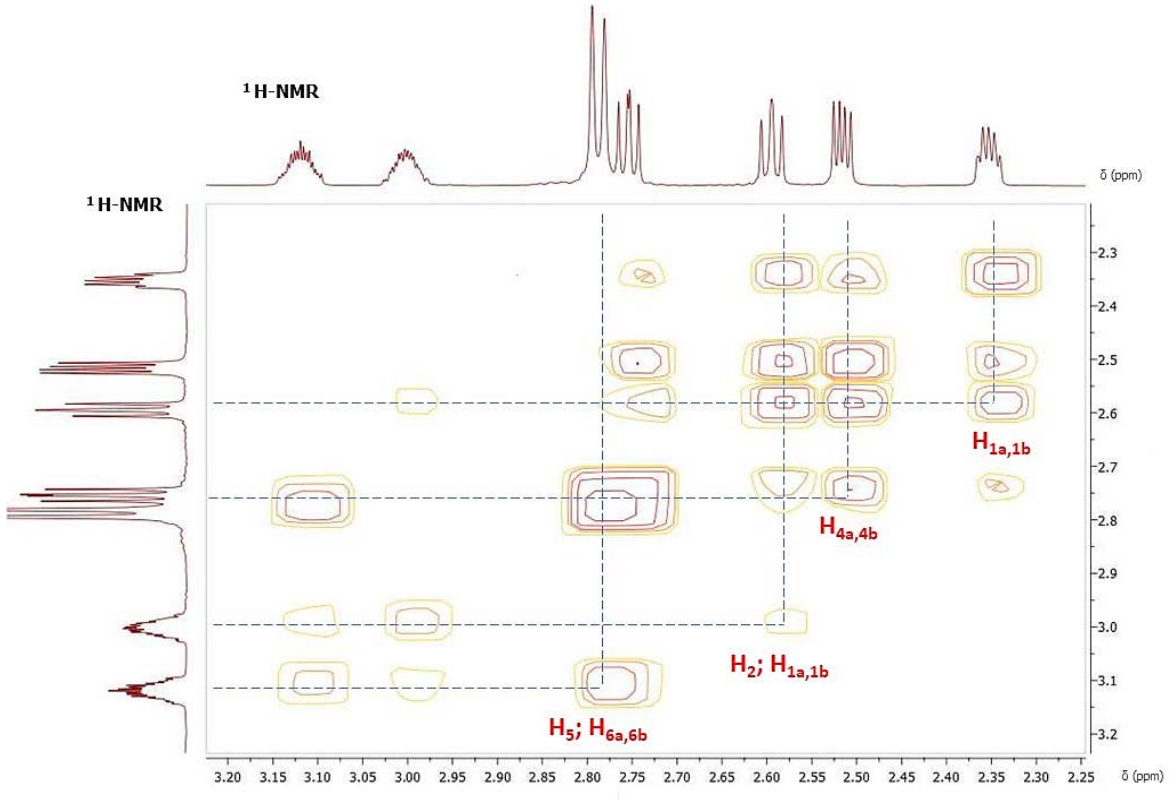

Figure 2. ^{1}H-^{1}H COSY spectrum of 4EPO-BEU in $CDCl_3$.

The signals in the ^{1}H NMR spectrum are rather complex due to the presence of four glycidyl groups, two of them directly linked to the aromatic ring, and other two, shielded at higher frequencies, due to their attachment to oxygen. Each glycidyl group has five non-equivalent protons due to the presence of the asymmetric carbon that leads the methylene protons to be diastereotopic to each other. Thus, five different signals are expected for each type of glycidyl group with a complex coupling pattern. The integration of signals and chemical shifts support the structure for 4EPO-BEU.

Figure 3 and 4 shows the ^{13}C NMR spectrum and HSQC NMR of the epoxy derivative with the corresponding assignments. The bidimensional spectrum allowed us the proper assignment of the signals to the corresponding carbon atoms in the structure, as they are detailed in the figures.

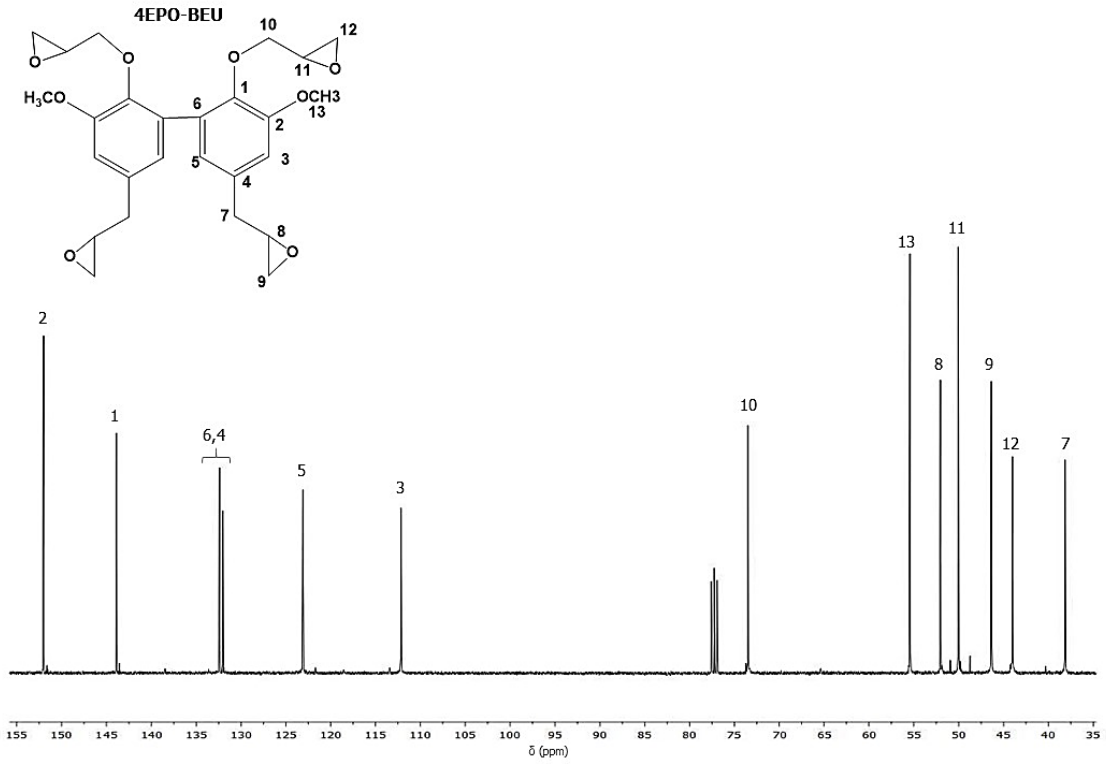

Figure 3. ^{13}C NMR spectrum of 4EPO-BEU in $CDCl_3$.

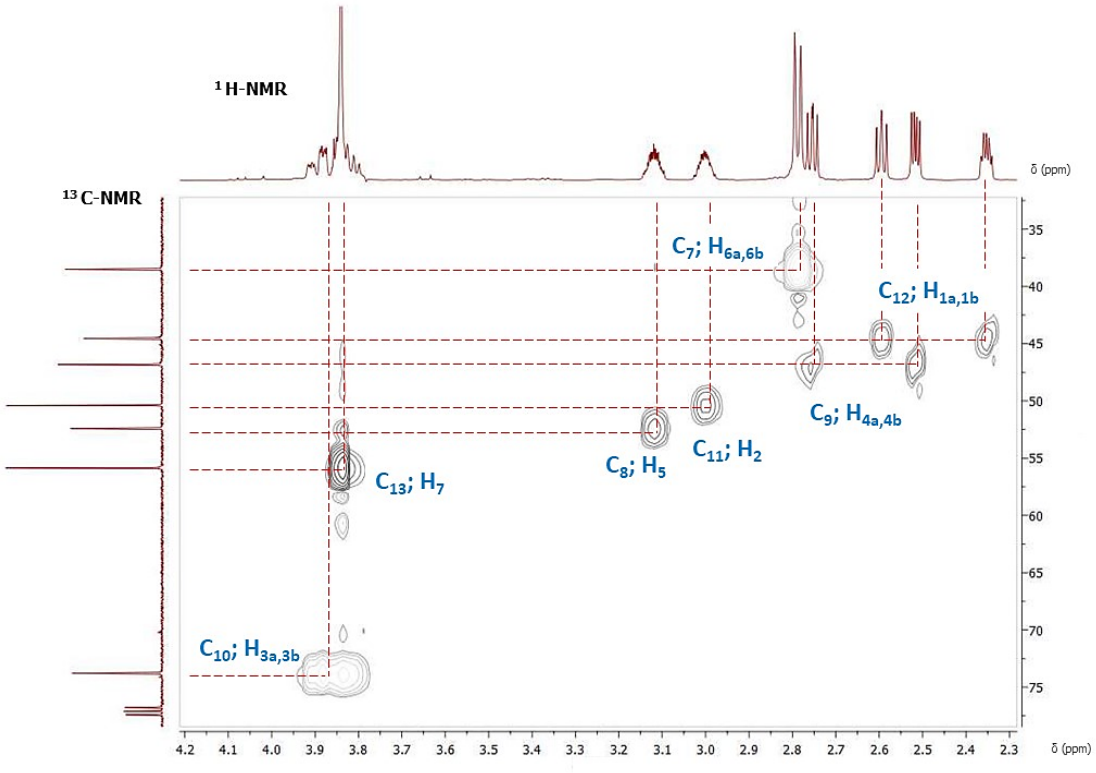

Figure 4. ^{1}H-^{13}C HSQC spectrum of 4EPO-BEU in $CDCl_3$.

The characterization of compounds derived from bis-eugenol by FTIR spectroscopy showed some characteristic absorptions corresponding to their chemical structures. In the figure 5 we can see the most relevant bands for the 4A-BEU, the vinyl stretching signal at 1638 cm^{-1}, and the absorptions at 833 cm^{-1} for 4EPO-BEU, which confirms the presence of both reactive groups.[34]

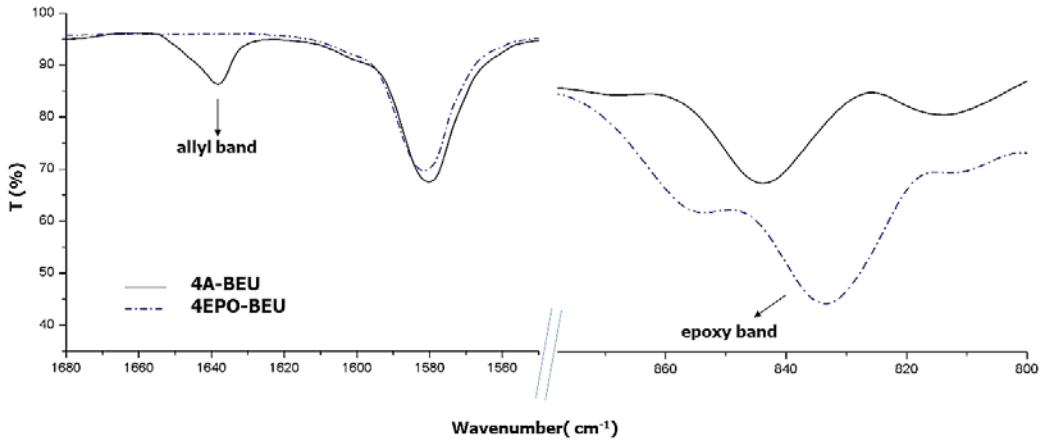

Figure 5. FTIR spectra of 4A-BEU and 4EPO-BEU.

The trithiol from eugenol (3SH-EU) and hexathiol derived from squalene (6SH-SQ) were synthesized by a two-step synthetic procedure, which consist in a first photochemical thiol-ene reaction followed by the saponification of thioester formed. The viscous liquids products were obtained with high yields and purity and the structures confirmed by spectroscopic measurements.[29,30] These thiols were described previously.

3.2. Preparation of materials based on 4A-BEU by thiol-ene reaction

The compound 4A-BEU and the different thiols were used as starting monomers in the preparation of thermosets by thiol-ene reaction using 4 phr of a 3:1 mixture of Irgacure 184/Irgacure 819 photoinitiators (PI), following a similar study carried out by

Yoshimura et al.[24] starting from a triallyl derivative of eugenol. In a previous work of our group, the thiol-ene reaction of eugenol derivatives was also deeply studied.[25]

The curing process of the thiol-ene formulations was followed by photoDSC and infrared spectroscopy. Figure 4 shows the exothermic curves corresponding to the isothermal photocuring of the formulations with the different thiols studied.

In the photoDSC plots it can be seen how the formulations 4A-BEU/ PETMP and 4A-BEU/ 3SH-EU are cured much faster than the formulation prepared with 6SH-SQ. This may be due to the different reactivity of primary and secondary thiol groups and to the fact that the hexathiol generates some topological restrictions that prevent the reaction from occurring properly. Although the shape of the curves does not allow an exact measurement of the reaction heat involved in this thiol-ene reaction, Table 1 shows the approximate heat evolved by gram of mixture or by equivalent of reactive group and the T_gs of the resulting materials.

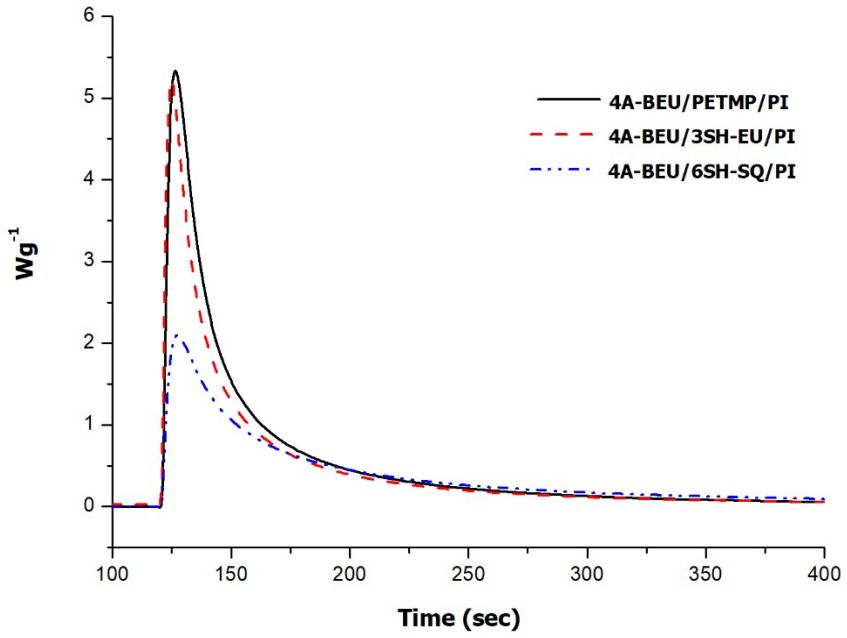

Figure 6. DSC thermograms corresponding to the photocuring at 30 °C of the mixtures of 4A-BEU with different thiols.

Table 2 reveals that the heat evolved in the photocuring of all formulations is a little lower than the reported by us in previous studies for thiol-ene processes, which were of about 50 kJ/eq.[35] In the case of the 6SH-SQ formulation, the enthalpy released per reactive group is lower than in the formulation with the tetrathiol or trithiol. This indicates that the reaction does not proceed completely, probably due to the above-mentioned topological restrictions produced by its multifunctional and compact structure. A similar behaviour was reported in other curing systems in which 6SH-SQ was involved.[25]

Table 2. Photocalorimetric and conversion data, obtained by FTIR spectroscopy, of the curing of all the formulations tested with 4 phr of photoinitiator mixture**.**

Formulation	ΔH[a] (J/g)	ΔH_{eq}[b] (kJ/eq)	T_g[c] (°C)	Allyl conversion[d] (%)	Thiol conversion[d] (%)
4A-BEU/PETMP	175	41	26	90	90
4A-BEU/3SH-EU	140	32	-6	70	100
4A-BEU/6SH-SQ	126	27	15	70	70

a. Enthalpy released per gram on irradiating the initial mixture
b. Enthalpy released per allyl equivalent on irradiating the initial mixture
c. Glass transition temperature of the final cured material
d. Conversion of both reactive groups determined by FTIR-ATR

The material prepared from the tetrathiol presented a higher T_g than materials prepared with 3SH-EU and 6SH-SQ. Although the multifunctionality of hexathiol and the stiffness of trithiol derived from eugenol should lead to higher T_g values, these thiols do not react completely, either due to topological problems, such as in the case of 6SH-SQ, or due to reactivity problems, such as 3SH-EU, as it was also observed in our previous study.[25]

To complete the curing study, the progress of the thiol-ene reaction was followed by FTIR spectroscopy to evaluate the real chemical transformation that takes place.

The evolution of the most significant bands of the starting monomers was followed by FTIR during irradiation of a film of the sample in the ATR. The evolution of the thiol groups was monitored by the band at 2570 cm^{-1} corresponding to S-H st and the decrease of the allyl groups by the band at 1638 cm^{-1} of the C=C st. As the reference band, we used the typical absorption of the aromatic ring at 1580-1600 cm^{-1}. The conversion was calculated as explained in the experimental part. Table 2 shows the final conversion reached of allyl and thiol groups in the cured material. As we can see, in the photochemical reaction of the 4A-BEU/PETMP mixture, allyl and thiol groups are consumed quasi completely in a parallel way. Yoshimura et al.[24] prepared materials from triallyl eugenol and tetrathiol (PETMP) by the same procedure and obtained a material with a T_g of 9.1 °C and very poor thermomechanical properties, similarly to that described by us.[25] They attribute the low curing degree achieved to undesired parallel reactions such as thiol-thiol coupling, which leads to a reduction of the crosslinking densities. Eugenol derivatives seem to present several problems when used in photochemical reactions. Its chemical structure, with allyl groups directly connected to an aromatic ring allows to stabilize radical species by means of resonance, reducing the reactivity of these allyl groups. This hypothesis can be confirmed by comparing our previous and present results. In triallyl eugenol derivatives,[25] with two allyl groups directly connected to the aromatic ring and an allyl ether, a conversion of 60% in the thiol-ene reaction with PETMP was reached. This is slower than in 4A-BEU, with two allyl groups directly attached to the ring but two ally ethers.

The formulation with the thiol derived from eugenol presents a thiol conversion of 100%, unlike the allylic group was consumed in an only 70%. The lower ally conversion

reached can be rationalized by the existence of thiol-thiol coupling during thiol-ene reaction, which has been reported before. [36] From the difference in the conversion of allyl and thiol groups, a 15% of this type of thiol-thiol linkage could be assumed. We reported in a previous paper that the 3SH-EU is not adequate for use in photochemical curing, since during the reaction,[34] thiyl radicals are formed which can react with each other. As a result, the materials obtained from 3SH-EU by photocuring processes present a very low T_g, as shown in Table 2. The occurrence of thiol-thiol coupling can lead to the formation of cycles, reducing the effective functionality of the thiol and consequently, the crosslinking density achieved and the T_g value.

In the case of the photocuring of 4A-BEU/6SH-SQ formulation allyl and thiol groups are consumed in a parallel way but reaching only a final conversion of 70%. Thus, thiol-thiol coupling seems not to proceed but the thiol-ene reaction may be limited by the lower reactivity and topological restrictions of squalene structure which agrees with the lower enthalpy evolved during photocuring.

3.3. Preparation of the materials derived from 4EPO-BEU by thiol-epoxy curing

In previous studies based on eugenol derivatives, we proved the greater suitability of thermal thiol-epoxy click processes in front of the photochemical thiol-ene reaction to obtain thermosets with good thermomechanical characteristics.[25] In addition, the tetrafunctionality of 4EPO-BEU leads us to expect even better performances.

The thiol-epoxy curing was studied by DSC to evaluate the evolution of the process with the different thiols, to find out the most adequate amine to catalyze the curing and the temperature range at which the curing occurs. In previous studies, we used 1-MI and DMAP as the base, being both adequate depending on the substrates

used.[25,30,34,35] The dynamic calorimetric curves obtained in the curing process of the different formulations are represented in Figure 7.

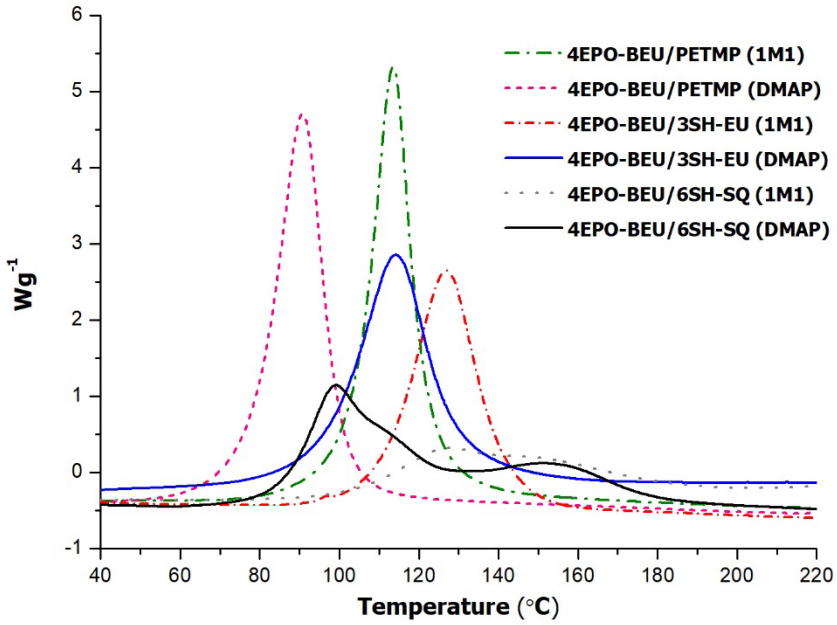

Figure 7. Calorimetric curves of the initial mixture 4EPO-BEU formulations with the thiols tested with 2 phr of the different catalysts.

As it can be seen, the mixture containing PTEMP shows the highest reactivity and the curing is produced at lower temperatures with a high curing rate. Differently, the formulations with 3SH-EU and 6SH-SQ react much slower, and the mixture with the hexathiol shows a very broad and bimodal curve that accounts for a lower reactivity, similarly to that observed before in the photochemical thiol-ene curing.

Between both catalysts, DMAP is more effective than 1-MI, since all the thiols initiate the curing at lower temperature with this catalyst. However, as our aim is to reach a certain stability of the initial formulation to be applied safely, we selected 1-MI as the catalyst. It should be also considered that 1-MI, which is liquid, is advantageous in front of the solid DMAP, in the preparation of homogeneous mixtures from the 4EPO-BEU based formulations, which are quite viscous. Table 3 collects the

relevant data of the curing process of these formulations. As we can see, the enthalpy released by epoxy equivalent is higher when PETMP is used as crosslinking agent, indicating that a higher degree of curing is achieved. In addition, the curing enthalpy, 126.7 kJ/eq, suggests that the reaction is complete, according to previously reported values.[37]

Table 3. Reaction enthalpies and T_gs determined by DSC of the different formulations studied, catalysed by 1-MI.

Formulation	**1-MI** (phr)	ΔH^a (J/g)	ΔH_{eq} [b] (kJ/eq)	T_g[c] (°C)
4EPO-BEU/PETMP	2	532	126.7	70
4EPO-BEU/3SH-EU	2	411	107.2	88
4EPO-BEU/6SH-SQ	2	187	42.0	47
4EPO-BEU/6SH-SQ	4	223	50.3	53
4EPO-BEU/6SH-SQ	8	378	86.2	57
4EPO-BEU	8	579	68.0	91

a. Enthalpy released per gram of sample in a dynamic curing
b. Enthalpy released per epoxy equivalent in a dynamic curing
c. Glass transition temperature of the final cured material

In the case of 4EPO-BEU/6SH-SQ formulations, the enthalpy released is very low and, therefore, we tried to increase the amount of 1-MI so that the curing process could reach full completion. Figure 8 shows the effect of the increasing amount of catalyst on the curing exotherms for the 4EPO-BEU/6SH-SQ formulations.

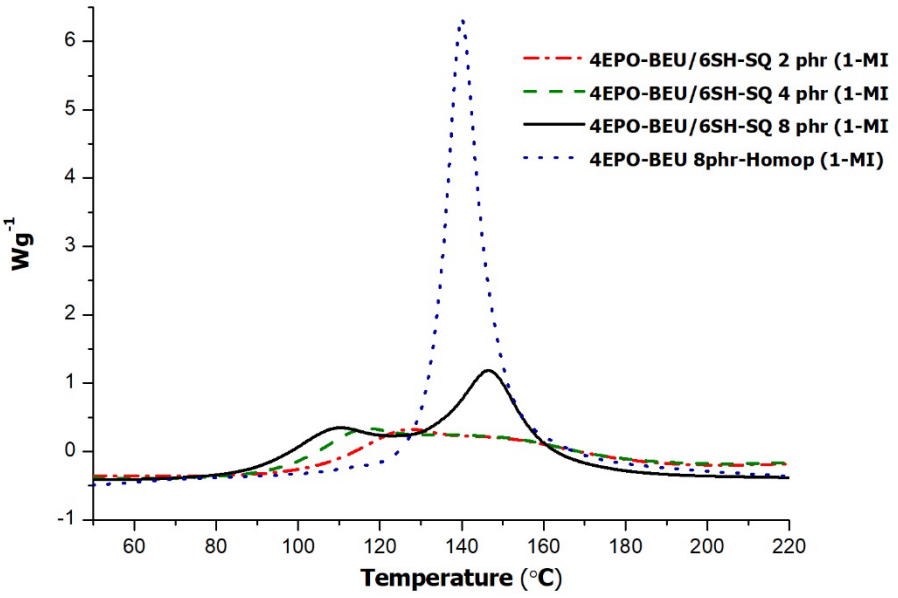

Figure 8. Calorimetric curves of the 4EPO-BEU/6SH-SQ formulations catalyzed by different proportions of 1-MI.

As can be seen in the figure, the amount of 1-MI markedly affects the curing process. As the amount of catalyst in the formulation increases, the presence of two polymerization processes becomes clearer. In the formulation with 8 phr of catalyst a bimodal curve with two maxima at about 110 °C and 145 °C are easily observable. The first exotherm can be assigned to the thiol-epoxy reaction, whereas the second peak, perfectly matches with the resin homopolymerization, also collected in Figure 7. The occurrence of epoxy homopolymerization in stoichiometric epoxy-thiol mixtures is explained by the low reactivity of 6SH-SQ and topological restrictions caused by the high density of thiol groups in the structure of 6SH-SQ, therefore limiting the extent of the thiol-epoxy reaction and leaving some unreacted epoxy groups. These groups are able to homopolymerize at higher temperature through an anionic ring-opening mechanism, initiated by 1-MI, as reported for non-stoichiometric thiol-epoxy formulations.[38] The limited extent of the thiol-epoxy reaction, resulting in the presence of unreacted thiol groups, indicates that the effective functionality of the 6SH-SQ co-

monomer is lower than expected. In a previous work, 6SH-SQ was used as curing agent of the triepoxy derivative of eugenol and a rather low curing degree was only achieved. The addition of a reactive diluent allowed attaining a higher degree of curing, which was explained on the basis of the reduction of steric and topological constrains.[34] The rigidity of 4EPO-BEU leads to a greater difficulty in reacting with the multifunctional and compact 6SH-SQ and therefore homopolymerization of epoxides becomes more important as side-reaction. In the figure, we can also see that on increasing the amount of catalyst the area under the second exotherm increases, as could be expected since higher proportions of imidazole generally enhance the reaction rate of the epoxy homopolymerization and promote a more complete cure and at lower temperatures.[39] In Table 3 the enthalpies evolved for all these formulations are collected. Although the addition of a higher amount of 1-MI to the formulation increases the heat released by epoxy equivalent, even with 8 phr of catalyst this value does not reach the one measured for 4EPO-BEU/3SH-EU and 4EPO-BEU/PETMP formulations catalyzed by 2 phr of imidazole. This is logical, in part, because the increase of the heat per epoxy equivalent is mainly due to the occurrence of the homopolymerization process. However, the homopolymerization of 4EPO-BEU does not rend the expected enthalpy per epoxy equivalent, which for DGEBA anionic homopolymerization was about 100 kJ/eq.[38,40] The lower curing degree achieved can be explained by the rigid and multifunctional structure of BEU epoxy derivative.

Table 3 collects the T_gs of the cured materials. Although PETMP introduces flexibility to the networked structure, the rigidity and high functionality of 4EPO-BEU leads to a T_g value (70ºC) that is clearly higher than that obtained for DGEBA/PETMP formulations, which resulted to be 55 °C.[37] Thus, from this point of view, bis-eugenol

derived epoxy monomer can be a perfect bio-based and safe substitute for DGEBA resins. Compared with the triepoxy derivative of eugenol,[34] the 4EPO-BEU presents a greater functionality, which allows increasing the T_gs of the thermosets from 60 to 70ºC. On increasing the rigidity of the thiol, the T_g is improved and the material obtained from 3SH-EU has a T_g of 88ºC.

In the case of 6SH-SQ, the increase in the proportion of 1-MI in the formulation produces an increase in the T_g of the materials obtained, as reported for epoxides cured with imidazole.[39] In spite of the low epoxy conversion reached, the thermoset obtained by the homopolymerization of 4EPO-BEU reached the highest T_g value. It should be commented that it is foreseeable that the use of 4EPO-BEU as bio-based and safe substitute of DGEBA resins can provide materials with T_g values higher or comparable when cured with traditional curing agents, such as amines or anhydrides.

FTIR-ATR analysis was performed to confirm the complete curing in 4EPO-BEU/PETMP formulations. Figure 9 shows the most significant regions of the spectra recorded before and after curing.

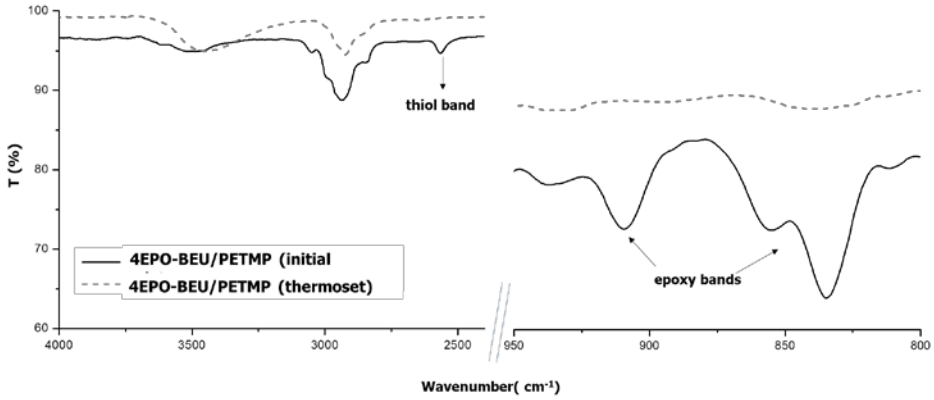

Figure 9. FTIR spectra of a mixture 4EPO-BEU/PETMP catalyzed by 2 phr of 1-MI before and after curing.

The initial spectrum shows the typical absorptions of S-H st. at 2570 cm^{-1} and the band at 908 and 835 cm^{-1} corresponding to the epoxy ring. These absorptions have disappeared completely in the spectrum of the cured material, whereas a new broad absorption at 3454 cm^{-1} appears because of the formation of the β-hydroxy thioether groups in the network structure. The small intensity of the thiol absorption and the overlapping of epoxide band with others in the region make difficult the monitoring of the evolution of the curing process, as previously reported.[38]

3.4. Characterization of materials based on 4A-BEU and 4EPO-BEU monomers

The materials prepared by thiol-ene and thiol-epoxy curing were characterized by different techniques to determine their thermal and mechanical characteristics.

The range of stability at high temperatures of the thermosets prepared was evaluated by thermogravimetry. Figure 10 shows the derivatives of weight loss curves against temperature in inert atmosphere and Table 4 collects the most significant data obtained by this technique.

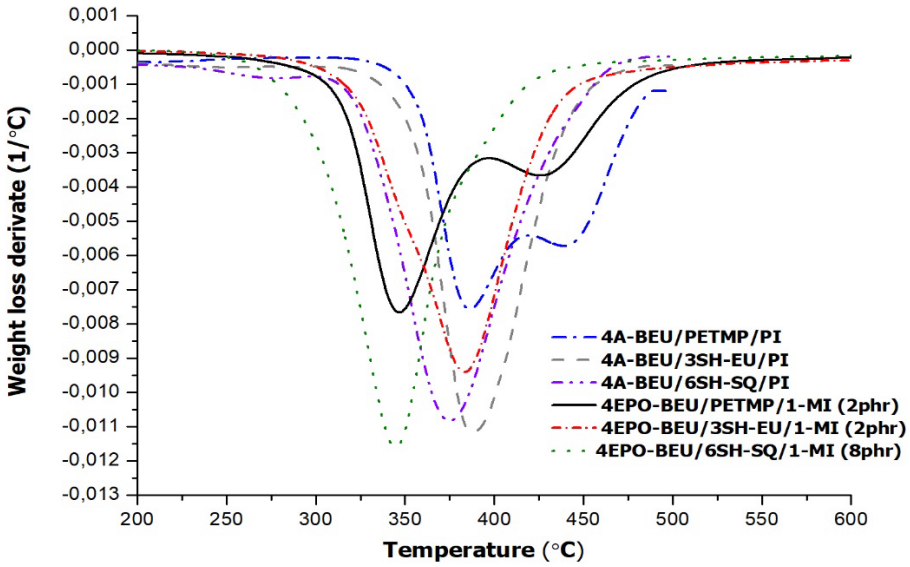

Figure 10. DTG curves under N_2 at 10 K/min of the materials obtained from bis-eugenol derivatives with different formulations by thiol-ene and thiol-epoxy curing.

At a glance, we can observe that the thermosets prepared from PETMP show a rather complex degradation mechanism. Regardless of the type of curing performed (photoinitiated thiol-ene or thermal thiol-epoxy), curves with a bimodal shape can be clearly observed, with a first and faster degradative process followed by a defined shoulder at temperatures above 400 °C. The higher complexity of degradation of the PETMP thermosets has been observed in similar materials obtained from 3EPO-EU and can be related to the presence of ester groups that degrade by a β-elimination process.[34] In contrast, the materials containing 3SH-EU and 6SH-SQ show unimodal degradation curves. The material prepared from the hexathiol begins to degrade at lower temperatures than the other thermosets.

Table 4. Thermal data of the materials obtained after curing processes from bis-eugenol derivatives.

Sample	$T_{5\%}$[a] (°C)	T_{max}[b] (°C)	$T_{tan\delta}$[c] (°C)	E_r[d] (MPa)	E[e] (MPa)
4A-BEU/PETMP	261	385	30	34.0	155
4A-BEU/3SH-EU	260	386	12	2.5	18
4A-BEU/6SH-SQ	240	374	29	7.0	72
4EPO-BEU/PETMP	311	347	83	26.0	1385
4EPO-BEU/3SH-EU	331	385	99	32.5	1970
4EPO-BEU/6SH-SQ	295	345	140	47.0	1606

a. Temperature of 5% of weight loss in N_2 atmosphere
b. Temperature of the maximum rate of degradation in N_2 atmosphere
c. Glass transition temperature determined by DMTA
d. Storage modulus in the rubbery state determined at δ + 50 °C
e. Young's modulus at 30 °C under flexural conditions

The values in the table show that the thermosets prepared from 6SH-SQ begin their degradation at lower temperatures than 3SH-EU or PETMP. The greater differences among all the materials were observed at the temperature of initial degradation ($T_{5\%}$). The materials cured by thiol-ene show a lower stability than those obtained by thiol-epoxy. This fact can be attributed to the lowest degree of curing attained. The temperature of higher rate of degradation is not affected significantly, although in thiol-epoxy thermosets seems to be a little lower. Although both type of

materials are similar from a structural point of view, thiol-ene thermosets have thioether bonds, whereas thiol-epoxy networks present β-hydroxy thioether units, which can contribute to produce different degradation patterns.

Table 4 collects the most typical thermomechanical data obtained for the materials prepared by thiol-ene and thiol-epoxy processes. We can see that cured materials by the photochemical process shows the lowest performance, as expected, due the lower degree of cure achieved. Among them, the material obtained from 4A-BEU/PETMP formulation shows the best thermomechanical characteristics, being higher than the previously reported materials obtained by photocuring of triallyl eugenol ($T_{tan\ \delta}$ 18ºC, E_r 6.7 MPa and Young's modulus 23.9 MPa).[25] Among triallyl eugenol derived thermosets, the best thermomechanical characteristics were reached when 6SH-SQ was the thiol selected, thanks to its multifunctionality that leads to a tighter network.[25] This is not the case in 4A-BEU materials. The differences observed in tri and tetra allyl eugenol derivatives can be due to the superior rigidity and bulky structure of the bis-eugenol core with a functionality of four that increase enormously the topological restrictions of the densely functionalized squalene hexathiol, leading to lower thiol-ene conversion that reduces the crosslinking density and consequently its thermomechanical behaviour. The use of 3SH-EU as the thiol leads to the softer and less crosslinked material in photocuring conditions, because of the coexistence of undesired side-reactions.[25]

On comparing the data of the thermally cured epoxy-thiol thermosets, it can be stated that the sample 4EPO-BEU/3SH-EU presents a slightly higher Young's modulus. 4EPO-BEU/6SH-SQ has the highest *tan δ* temperature, but this result can be only attributed to the contribution of the structures formed by homopolymerization,

randomly distributed in the network, which are tighter and not to the desired thiol-epoxy curing process, which as demonstrated previously was not complete.

When compared the thermomechanical data obtained for 4EPO-BEU/PETMP and DGEBA/PETMP thermosets[37] we can confirm that the bis-eugenol derivative is a good alternative for replacing the oil-derived DGEBA resin. The use of thiols obtained from natural sources allow to obtain a series of 100% renewable thermosets.

In addition to the values obtained from thermomechanical tests, it is interesting to examine the α relaxation curves of the materials prepared. Figure 11 shows the curves of the different materials obtained.

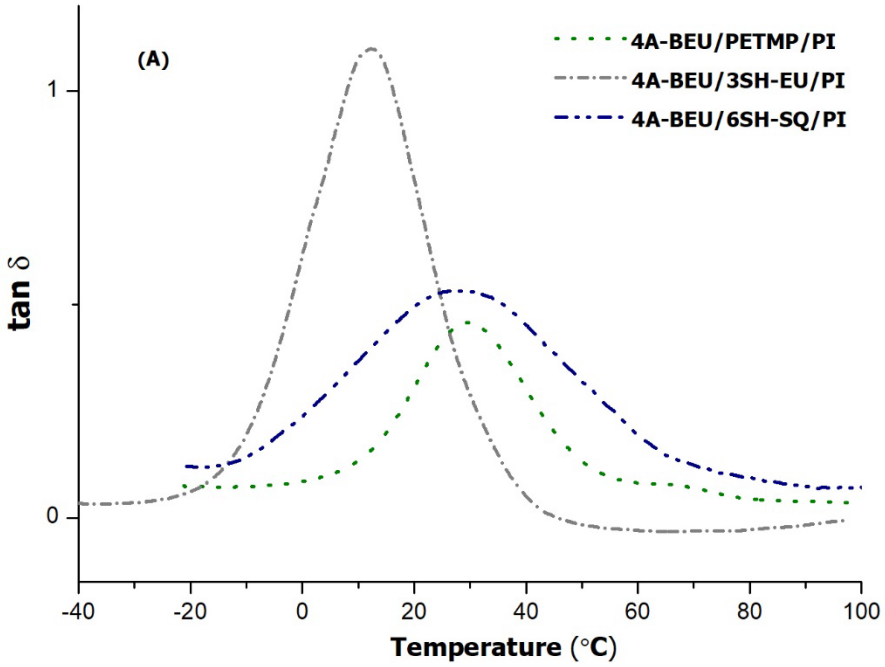

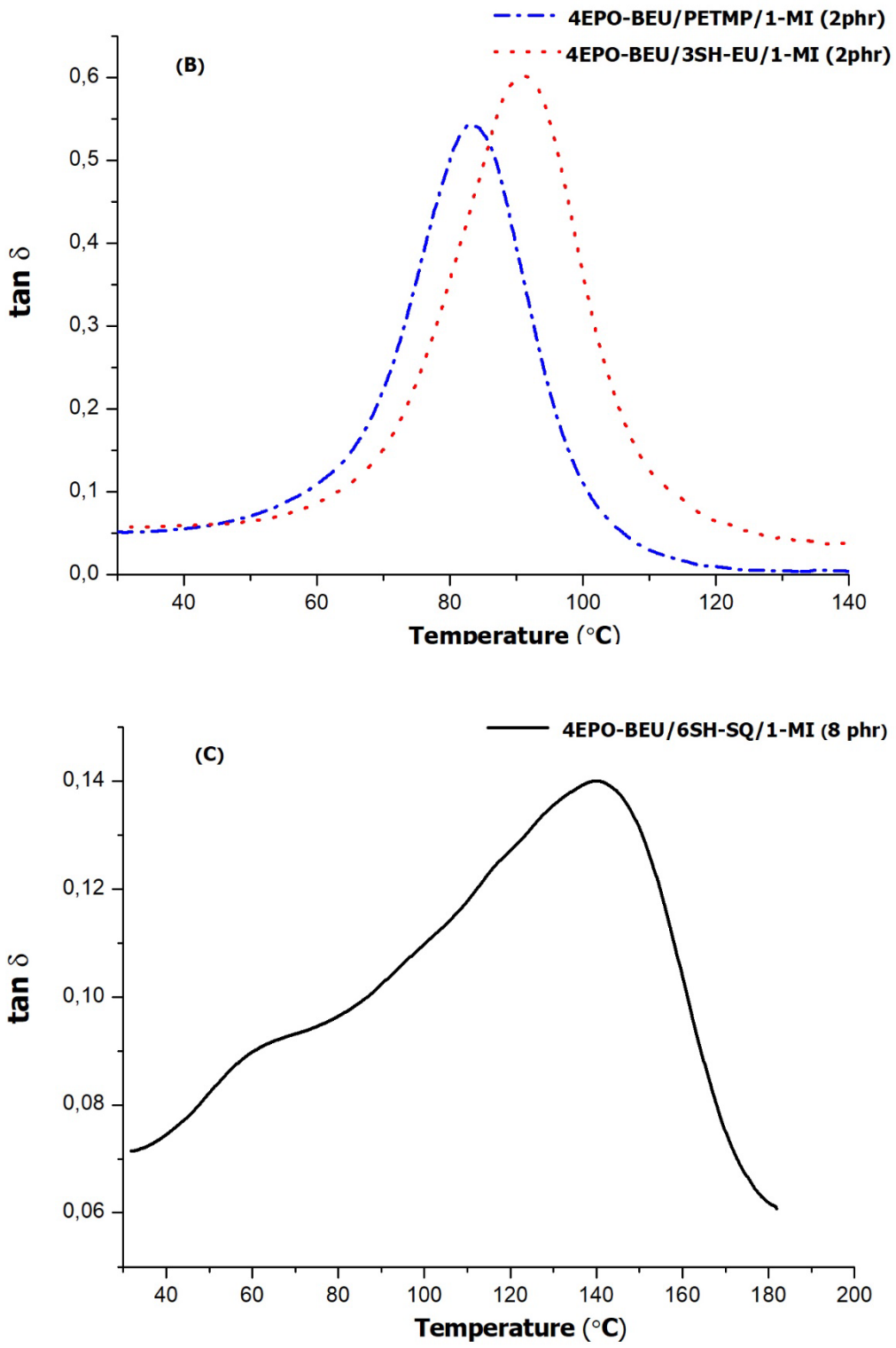

Figure 11. Plots of *tan δ* against temperature for the various materials prepared.

The *tan δ* curves of the materials obtained by photopolymerization are broader (plot A), as the result of the occurrence of side-reactions in the thiol-ene process and

to the uncomplete curing achieved, both facts increasing the heterogeneous character of the materials. However, the material obtained from PETMP as the thiol seems to have a higher homogeneity, according to the better performance of thiol-ene reaction in this system (Table 2). In reference to the thiol-epoxy materials, the shape of the curves of 4EPO-BEU/PETMP and 4EPO-BEU/3SH-EU (plot B) samples are unimodal and narrow. In contrast, the material 4EPO-BEU/6SHSQ (plot C) leads to a broad and bimodal *tan δ* curve. This suggests there is a significant network heterogeneity and indicates the coexistence of two clearly different network structures in the material, one from thiol-epoxy reaction (evidenced by the shoulder at 60-70 ºC) and another from a polyether network (evidenced by the peak at 140 ºC). The shape and size of the *tan δ* curve also indicate that the mobility of the network is severely restricted due to the tightly crosslinked network structure caused by the homopolymerization process and the rigid structure of the bis-eugenol backbone.

From the thermomechanical characterization, it is clear that for bis-eugenol structures, thermal thiol-epoxy processes are more effective than photochemical thiol-ene reactions to get materials with better mechanical performance. This observation agrees well with the results obtained in simple eugenol derivatives[25] and confirms that the eugenol structure is not fully adequate for radical type thiol-ene reactions.

The strain-stress and hardness measurements (microindentation Vickers hardness for 4EPO-BEU samples and Shore hardness for 4A-BEU samples) testing were performed on all the samples to evaluate the mechanical characteristics of the materials prepared. Table 5 collects the main data extracted from these tests.

Table 5. Mechanical data obtained by stress-strain and hardness testing of the materials prepared. Coefficients of variation less than 5% for stress, strain and tensile modulus, and less than 3% for hardness results.

Sample	Strain at break (%)	Stress at break (MPa)	Microindentation hardness[a,b] (HV)	Shore hardness[c]
4A-BEU/PETMP	20.5	5.1	---	50*
4A-BEU/3SH-EU	28.6	0.4	---	50**
4A-BEU/6SH-SQ	39.2	1.9	---	78**
4EPO-BEU/PETMP	3.1	25.5	11.5	---
4EPO-BEU/3SH-EU	2.9	33.9	12.8	---
4EPO-BEU/6SH-SQ	1.6	29.9	14-20	---

a. Indentation test load of 10 g for formulations: 4A-BEU/PETMP, 4EPO-BEU/3SH-EU and 4A-BEU/6SH-SQ
b. Indentation test load of 25 g for formulations: 4EPO-BEU/PETMP and 4EPO-BEU/6SH-SQ
c. Shore hardness test with a durometer Type D (*) for 4A-BEU/PETMP and Type A (**) for 4EPO-BEU/3SH-EU and 4A-BEU/6SH-SQ.

As can be seen, the materials obtained by photochemical curing have lower tensile strength and higher elongation at break, showing an elastomeric behaviour. The material prepared using 4A-BEU/PETMP show the best characteristics in Young's modulus (Table 4) and strength at break, related to the fact that it is the only one that has a T_g close to room temperature (26ºC by DSC, Table 2), in contrast to the other materials which clearly are in the rubbery state. Among 6SH-SQ and 3SH-SQ samples, the material obtained from 6SH-SQ presents the best resistance at break in terms of stress and strain in agreement with the results presented for Young's modulus.

The thermosets obtained by thermal curing present a significant increase in the tensile strength and a decrease in the elongation at break in reference to the photoirradiated. The rigid character of these materials leads to a very small strain at break according to their higher crosslinking degree, being the lowest the one of the 4EPO-BEU/6SH-SQ material due to the contribution of the polyether network.

Epoxy-thiol derived materials exhibited higher hardness values than the materials obtained by thiol-ene curing, as expected. As commented in the experimental section,

due to the elastomeric nature of 4A-BEU samples, Vickers microindentation hardness test was not a suitable technique because of the uncertainty in the measurement of the surface area of the indentation due to the elastic recovery process. Therefore, the Shore hardness test was used for 4A-BEU materials, with the scale A (Shore A hardness with lower penetration load for softer materials) for 3SH-EU and 6SH-SQ samples and the scale d (Shore D hardness with higher penetration load for harder materials) for PETMP samples. Table 4 shows that the material prepared form the mixture 4A-BEU/3SH-EU presented the lowest hardness value in accordance to its low value of T_g (12ºC) and Young's modulus (18 MPa). On the contrary, sample 4A-BEU/PETMP presented the highest hardness in agreement to its highest Young's modulus.

Microindentation hardness for 4EPO-BEU/PETMP and 4EPO-BEU/3SH-EU samples presents similar values, slightly higher for the later one, as expected looking at their Young's moduli. The inhomogeneous character of the 4EPO-BEU/6SH-SQ thermoset becomes also evident from the determination of the hardness, with values between 14 and 20, being 20 the most predominant in the material, according to the prominent polyether structure in the network.

4. Conclusions

Two different tetrafunctional compounds, 4A-BEU and 4EPO-BEU, were prepared from bis-eugenol, previously obtained by dimerization of eugenol as starting renewable material. The synthetic procedure consisted in an allylation reaction and further epoxidation using oxone to obtain the epoxy derivative.

The tetra allyl derivative of bis-eugenol, 4A-BEU, was used as the ene-monomer in the thiol-ene reaction using different thiols: PETMP, that can be obtained from

natural sources, and two thiols, 3SH-EU and 6SH-SQ, synthesized by us from renewable sources such as eugenol and squalene. Photocuring of these mixtures produces incomplete curing and side-reactions that limits the degree of curing achieved. PETMP led to a more complete cure in comparison with 3SH-EU and 6SH-SQ.

The tetraepoxy derivative of bis-eugenol, 4EPO-BEU, was reacted in the thiol-epoxy reaction with the previous thiols. 1-Methylimidazole was used as catalyst. The curing with PETMP and 3SH-EU was complete, but 6SH-SQ led to a limited degree of curing and homopolymerization of epoxide at high temperature also occurred.

The materials prepared from the thiol-epoxy curing had better thermal and mechanical characteristics than the materials obtained by photochemical thiol-ene reaction, but the thermoset's network from squalene has a heterogeneous character.

The thermosets of the present study can be considered as 100% bio-based. Bis-eugenol compounds are advantageous in front of simple eugenol derivatives previously reported. Finally, it should be pointed out, that the tetra epoxy bis-eugenol derivative constitutes a safe and valuable bio-based alternative for replacing high-performance oil-derived DGEBA in the preparation of epoxy thermosets.

Acknowledgments

The authors would like to thank MINECO (Ministerio de Economia, Industria y Competitividad, MAT2017-82849-C2-1-R and -2-R) and to Generalitat de Catalunya (2017-SGR-77 and Serra-Húnter programme) for the financial support.

Conflicts of interest

There are no conflicts to declare.

References

1 R. Mülhaupt, *Macromol. Chem. Phys.* 2013, **214,** 159−174.

2 R. Auvergne, S. Caillol, G. David and B. Boutevin, *Chem. Rev.* 2014, **114**, 1082−1115.

3 M. Stemmelen, V. Lapinte, J-P Habas and J-J Robin, *Eur. Polym. J.* 2015, **68**, 536–545.

4 C. Ding, P. S. Shuttleworth, S.Makin, J. H. Clark and A. S. Matharu, *Green Chem.* 2015, **17**, 4000-4008.

5 S. Kumar, S. Krishnan, S. Mohanty and S. K. Nayak, *Polym. Int.* 2018, **7**, 815-839.

6 M. Fache, B. Boutevin and S. Caillol, *ACS Sustainable Chem. Eng.* 2016, **4,** 35−46.

7 E. Savonnet, E. Grau, S. Grelier, B. Defoort and H. Cramail, *ACS Sustainable Chem. Eng.* 2018, **6,** 11008−11017.

8 S. Ma, X. Liu, Y. Jiang, Z. Tang, C. Zhang and J. Zhu, *Green Chem.* 2013, **15**, 245–254.

9 E. Darroman, N. Durand, B. Boutevin and S. Caillol, *Prog. Org. Coat.* 2016, **91**, 9–16.

10 F. Hu, J. J. La Scala, J. M. Sadler and G. R. Palmese, *Macromolecules*, 2014, **47**, 3332−3342.

11 P. Niedermann, G. Szebényi, and A. Toldy, *Express Polym. Lett.* 2015, **9**, 85–94.

12 G. Wenqiang, L. Shufen, Y. Ruixiang, T. Shaokun, and Q. Can, *Food Chem.* 2007, **101**, 1558–1564.

13 B. Yogalakshmi, P. Viswanathan and C.V. Anuradha, *Toxicology*, 2010, **268**, 204–212.

14 A. Garg, S. Singh, *Colloid Surf., B*, 2011, **87**, 280–288.

15 H. J. Bohnert, H. R. Nguyen and N.G. Lewis, *Bioengineering and Molecular Biology of Plant Pathways*, Elsevier, CA, USA, San Diego, 2008.

16 G. P. Kamatou, I. Vermaak and A. M. Viljoen, *Molecules*, 2012, **17**, 6953-6981.

17 Expert Committee on Food Additives, *Evaluation of Certain Food Additives and Contaminants*, WHO Technical Report Series 683, WHO Press: Genève, Swiss, 1982.

18 T. S. Kaufman, *J. Braz. Chem. Soc.*, 2015, **26**, 1055-1085.

19 Y. Zhang, Y. Li, V. K. Thankur, Z. Gao, J. Gu and M. R. Kessler*, Polym. Int.* 2018, **67**, 544-549.

20 J. Qin, H. Liu, P. Zhang, M. Wolcott and J. Zhang, *Polym. Int.* 2014, **63**, 760-765.

21 J. Wan, B. Gan, C. Li, J. Molina-Aldareguia, E. Naderi Kalali, X. Wang and D-Y Wang, *Chem. Eng. J.* 2016, **284**, 1080–1093.

22 J. Wan, J. Zhao, B. Gan, C. Li, J. Molina-Aldareguia, Y. Zhao, Y-T Pan and D-Y Wang, *ACS Sustainable Chem. Eng.*, 2016, **4,** 2869−2880.

23 T, Liu, C. Hao, L. Wang, Y. Li, W. Liu, J. Xin and J. Zhang, *Macromolecules,* 2017, **50**, 8588-8597.

24 T. Yoshimura, T. Shimasaki, N. Teramoto and M. Shibata, *Eur. Polym. J.* 2015, **67**, 397–408.

25 D. Guzmán, X. Ramis, X. Fernández-Francos, S. De la Flor and A. Serra, *Eur. Polym. J.* 2017, **93**, 530-544.

26 A. De Farias Dias, *Phytochemistry*, 1988, **27**, 3008-3009.

27 D. Fourcade, B. Sebastian Ritter, P. Walter, R. Schönfeld and R. Mülhaupt, *Green Chem.* 2013, **15**, 910-918.

28 M. Neda, k. Okinaga, M. Shibata, *Mater. Chem. Phys.* 2014, **148**, 319-327.

29 R. Acosta Ortiz, E.A. Obregón Blandón and R. Guerrero Santos, *Green Sustainable Chem.* 2012, **2**, 62-70.

30 D. Guzmán, B. Mateu, X. Fernández-Francos, X. Ramis and A. Serra, *Polym. Int.* 2017, **66**, 1697-1707.

31 B. Kim, J. Young Kim, Y. Yi and Y. Lim, *J. Korean Soc. Appl. Biol.* 2012, **55**, 677-680.

32 N. Hashimoto and A. Kanda, *Org. Process Res. Dev.* 2002, **6**, 405-406.

33 C. Aouf, H. Nouailhas, M. Fache, S. Caillol, B. Boutevin and H. Fulcrand, *Eur. Polym. J.* 2013, **49**, 1185-1195.

34 D. Guzmán, X. Ramis, X. Fernández-Francos, S. De la Flor and A. Serra, *Prog. Org. Coat.* 2018, **114**, 259-267.

35 D. Guzmán, X. Ramis, X. Fernández-Francos and A. Serra, *RSC Adv.* 2015, **5**, 101623-101633.

36 S.P.S. Koo, M.M. Stamenovic, R.A. Prasath, A.J. Inglis, F.E. Du Prez, C. Barner-Kowollik, W. Van Camp and T. Junkers, *J. Polym. Sci. Part A: Polym. Chem.* 2010, **48**, 1699–1713.

37 D. Guzmán, X. Ramis, X. Fernández-Francos and A. Serra, *Polymers*, 2015, **7**, 680-694.

38 X. Fernández-Francos, A-O. Konuray, A. Belmonte, S. De la Flor, A. Serra and X. Ramis, *Polym. Chem.* 2016, **7**, 2280-2290.

39 M. S. Heise, G. C. Martin, *Macromolecules*, 1989, **22**, 99-104.

40 X. Fernández-Francos, W. D. Cook, A. Serra, X. Ramis, G. G. Liang and J. M. Salla, *Polymer*, 2010, **51**, 26-34.